


 Cite this: *RSC Adv.*, 2021, **11**, 11356

## Synthesis and evaluation of the oil removal potential of 3-bromo-benzimidazolone polymer grafted silica gel†

 Oisaemi Uduagele Izevbekhai, <sup>\*a</sup> Wilson Mugera Gitari, <sup>\*a</sup> Nikita Tawanda Tavengwa, <sup>b</sup> Wasiu Babatunde Ayinde<sup>a</sup> and Rabelani Mudzielwana<sup>a</sup>

This work reports the synthesis of 3-bromo-benzimidazolone using melt condensation, its polymerization and functionalization on silica which was extracted from diatomaceous earth in our previous work. The synthesized compounds were characterized using FTIR, NMR, SEM-EDS and TEM. The FTIR and NMR spectra of the synthesized benzimidazolones showed the compounds to have several functional groups: A band due to Si–O–C at 1085.41 cm<sup>-1</sup>, a broad band at 3380 cm<sup>-1</sup> and chemical shifts: positive distortionless enhancement by polarization transfer (DEPT) <sup>13</sup>C peaks (indicating lack of CH<sub>2</sub> and CH<sub>3</sub> groups), <sup>1</sup>H NMR – 11.053 ppm (N–H), 7.086 ppm (Ar–H); <sup>13</sup>C NMR – 155.34 ppm (C=O), 101.04 ppm (C–Br) characteristic of benzimidazolones. SEM-EDS of the functionalized silica showed a rough irregular morphology with Si and O as the major elements. Carbon was also present indicating that silica was successfully functionalized with 3-bromo-benzimidazolone and TEM showed interconnected smear-like particles arranged irregularly. The functionalized silica was then applied in the treatment of oily wastewater and factors like initial oil concentration, adsorption dosage and time were optimized using the central composite design of response surface methodology in the design expert software. The amount of oil adsorbed was obtained by quantifying the total organic carbon using TOC test kits. Results showed that the optimum conditions for oil removal were 6650 mg L<sup>-1</sup> oil concentration, with adsorbent dosage of 0.004 g and a contact time of 16 h. Under these conditions, the percentage adsorption was 97.9% with a desirability of 0.99. The materials were therefore seen to be applicable to field wastewaters.

 Received 26th December 2020  
 Accepted 8th March 2021

 DOI: 10.1039/d0ra10848k  
[rsc.li/rsc-advances](http://rsc.li/rsc-advances)

### Introduction

Petroleum is widely used globally, and its use is predicted to increase to about 107 million barrels daily by the year 2030. The exploration of this mineral requires a lot of water<sup>1,2</sup> just like all fossil fuel extraction and generates wastewater very rich in oils.<sup>1</sup>

Oily wastewater is ranked high in the global environmental issues list, hence treating it is of paramount importance.<sup>3-4</sup> Coagulation, filtration with coagulation, precipitation, ozonation, ion exchange, reverse osmosis, biological methods and advanced oxidation processes have been used to treat oily wastewater in the past, but these methods have technical and economic limitations.<sup>5-9</sup>

Adsorption is another method that has been used in the treatment of oily wastewater with advantages over other methods such as, high removal efficiency, low energy demand, less chemical investment and reusability.<sup>10</sup> Over the years, several adsorbents like activated carbon, zeolites, coal, fly ash, clays and nanomagnetic particles have been used. Moazed *et al.*<sup>11</sup> used bentonite clay to remove oil from water and reported 70% adsorption of its weight in oil. It was also reported that the bentonite clay material had an oil removal capacity of 100%, but the materials were not successful in the removal of organic particles.<sup>11</sup> The other adsorbents listed above were found to have relatively low adsorption capacities.<sup>2,10</sup> Fly ash was reported to have an oil removal efficiency of 70–80% and the adsorption data obtained in this study, fitted best to Freundlich isotherm indicating adsorption on a heterogenous surface.<sup>12-14</sup> Li *et al.*<sup>3</sup> used different particle sizes of three different types of coal – anthracite, lean coal and lignite to remove oil from wastewater. The results of their experiments indicated that the quantity of absorbed oil decreased with an increase in particle size. They also found anthracite to have the highest adsorption capacity (24.4 mg g<sup>-1</sup>). Since the first synthesis of porous silica gels in 1968,<sup>15</sup> different porous gels

<sup>a</sup>Environmental Remediation and Nano Sciences Research Group, School of Environmental Sciences, University of Venda, Private Bag X5050, Thohoyandou 0950, South Africa. E-mail: gitariw@gmail.com; oisaemii@gmail.com

<sup>b</sup>Department of Chemistry, University of Venda, Private Bag X5050, Thohoyandou 0950, South Africa

† Electronic supplementary information (ESI) available. See DOI: 10.1039/d0ra10848k



with different modifications and pore sizes have been synthesized by modifying the reaction conditions and parameters.<sup>16</sup> This makes the materials potentially applicable in a wide range of areas. The modifications have recently been extended to organic polymers giving the materials characteristics of both organic and inorganic moieties.<sup>12,13,17</sup>

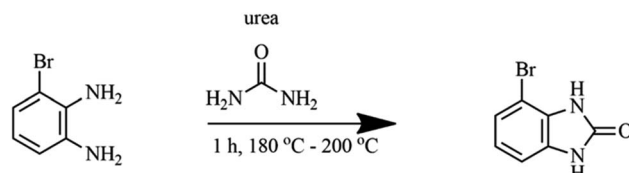
The benzimidazole group is an integral part of many therapeutic agents with many known applications as antiviral, anti-histaminic, selective nucleotide-binding oligomerization domain-containing protein 1 and angiotensin-converting-enzyme inhibitory agents.<sup>18</sup> Benzimidazol-2-ones are an important group of benzimidazoles and have been applied as antipsychotic, antihistaminic, antihypertensive anti-trichinellosis agents and antiviral agents, among others.<sup>19</sup> This group of compounds have only been applied in a few instances in remediation of wastewater. For example, Samai *et al.*<sup>20</sup> successfully applied bis-benzimidazole compounds in the sorption of dyes and its derivatives have been shown to be good adsorbents of acids.<sup>21</sup>

Given the frequency of use of petroleum products and the associated spills and the increasing scarcity of water, there is need for a reliable and efficient adsorbent to remove oil from water. This work was aimed at the synthesis of 3-bromobenzimidazolone derivatives of porous silica gels which has never been investigated before. A closely related compound, benzimidazoles, have however shown excellent sorption properties because of the numerous functional groups it presents. 3-Bromobenzimidazolone was chosen over the benzimidazoles for this work because it presents an additional functional group, the carbonyl group which is potentially useful in oil sorption. The synthesis was carried out by first synthesizing the benzimidazolone through a solvent free process followed by its copolymerization with silica. For the first time, the usability of these benzimidazolone–silica hybrids in the treatment of oily wastewater is reported. The removal of oil from water using these adsorbents were optimized using response surface methodology and the optimum conditions for oil removal were obtained using this software.

## Experimental

### Chemicals and reagents

Silica extracted from diatomaceous earth in our previous study was used after drying.<sup>22,23</sup> Sodium dodecyl sulphate, 3-bromo-1,2-benzenediamine, urea and ammonium persulphate were of analytical grade and obtained from Sigma-Aldrich (St Louis, USA), NaOH and HCl was obtained from Rochelle Chemicals (Johannesburg, South Africa). Milli-Q water from Millipore S.A.S (Molsheim, France) ( $18.2 \mu\text{s cm}^{-1}$  at  $25^\circ\text{C}$ ) was also used in all dilutions. Tea bags were bought from Shoprite, Thohoyandou, South Africa. Vacuum pump oil was from Telstar technologies (Barcelona, Spain). Freeze dryer (Telstar Lyoquest-55, Shanghai, China) was used to freeze dry samples and spectrophotometer (Merk Group, Germiston, South Africa) was used for total organic carbon measurement and Stuart reciprocating shaker (Staffordshire, UK) was used for shaking and



Scheme 1 Synthesis of 3-bromo-benzimidazolone.

functional group analysis was carried out using an ALPHA FT-IR spectrophotometer from Bruker Pty (Sandton, South Africa).

Synthetic oily wastewater (SOWW) was prepared by modifying the method described by Shoba *et al.*<sup>24</sup> Sodium dodecyl sulphate and vacuum pump oil (90 : 1 v/w) were added to a 1 L flask and the volume made up with water. The mixture was then sonicated for 5 min at an amplitude of 75% and cycle of 0.5 to make the mixture homogenous.

### Synthesis of benzimidazolone

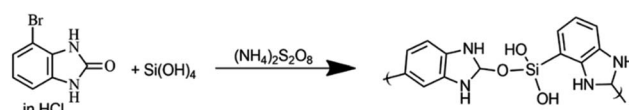
Benzimidazolone were prepared by modifying the method described by Mavrova *et al.*,<sup>25</sup> Izevbekhai *et al.*<sup>26</sup> and Yang *et al.*<sup>27</sup> 1 mole of 3-bromo-1,2-benzenediamine, was mixed thoroughly with 1 mole of urea by crushing in a mortar and heated at  $190^\circ\text{C}$  for 1 h over a sand bath as shown in reaction Scheme 1. The resulting solute was allowed to cool to room temperature and dissolved in 10% NaOH, filtered and the filtrate extracted with 35% HCl, filtered, dried and then characterized using FT-IR and NMR.

### Polymerization of 3-bromo benzimidazolone

Prepared 3-bromo-benzimidazolone was polymerized by modifying the method described by Mdlalose *et al.*<sup>28</sup> Silica and benzimidazolone (mole ratio 2 : 1) were dissolved in 50 mL, 0.1 M HCl and stirred in a beaker over ice bath for 3 h. A volume of 25 mL 0.6 M ammonium persulphate in HCl was then added dropwise into the reaction mixture and stirring was continued for 24 h (Scheme 2). The reaction was then quenched by the addition of acetone and filtered. The filtrate was evaporated to dryness at  $60^\circ\text{C}$  to obtain solutes which were characterized and used in adsorption experiments.

### Response surface optimization of oil removal

The synthesized polymer was used in the optimization tests as described by Izevbekhai *et al.*<sup>29,30</sup> Variable amounts of adsorbent were put in sealed tea bags and placed in a constant volume of SOWW. To test the effect of the tea bags, empty tea bags were sealed and used in similar experiments. The setup was allowed to stand for some time. After this, the solution was filtered and



Scheme 2 Polymerization of 3-bromo benzimidazolone.



Table 1 Range of optimized parameters

Parameter	Low	High
Oil concentration (mg L <sup>-1</sup> )	192	9250
Sorbent dosage (g)	0.0011	0.004
Contact time (h)	16.0	60.5

the TOC of the treated and untreated SOWW was measured using a spectroquant UV spectrophotometer. The percentage oil removal was calculated using eqn (1).

$$\% \text{ removal} = \left( \frac{(C_i - C_f)}{C_i} \times 100 \right) \quad (1)$$

where  $C_i$  and  $C_f$  are the oil concentrations (mg L<sup>-1</sup>) before and after treatment with adsorbent respectively.

## Experimental design

Percentage oil removal was optimized by varying the weight of 3-bromo benzimidazolone polymer, initial oil concentration and contact time using the central composite design in the response surface methodology (RSM) software. The range of optimized parameters are listed in Table 1.

## Results and discussion

### Functional group analysis

Fig. 1 shows the FT-IR spectra of 3-bromo-1,2-diaminobenzene, urea and the synthesised 3-bromo-benzimidazolone. The spectrum for 3-bromo-1,2-diaminobenzene exhibited bands at 620 cm<sup>-1</sup> due to C-Br, 797 cm<sup>-1</sup>, 1060 cm<sup>-1</sup> (CH out of plane), 1234 cm<sup>-1</sup>, 1295 cm<sup>-1</sup> (CH plane), 1367 cm<sup>-1</sup>, 1625 cm<sup>-1</sup> (C-N stretching vibration), 1456 cm<sup>-1</sup>, 1573 cm<sup>-1</sup> and 1738 cm<sup>-1</sup> (aromatic C=C) as well as 3282 cm<sup>-1</sup> and 3371 cm<sup>-1</sup> due to N-H bonds. The product (3-bromo-benzimidazolone) showed

distinctive bands, for example, the bands at 1458 cm<sup>-1</sup> and 1599 cm<sup>-1</sup> are characteristic of the C=C stretching of the benzene ring,<sup>31</sup> band at 3117 cm<sup>-1</sup> is characteristic of N-H stretching bands of benzimidazoles.<sup>32</sup> This band was seen to be broad probably due to OH groups formed as a result of tautomerism in the benzimidazolone ring and also as a result of intra-molecular hydrogen bonding.<sup>33</sup> Also worthy of note was the fact that the band for asymmetric N-H stretching seen in the spectrum for 3-bromo-1,2-diaminobenzene, was absent in the 3-bromobenzimidazolone spectrum because the primary NH<sub>2</sub> group (amine) in the former becomes a secondary NH group (amine) in the later. There was also an observed red shift in band for the C=O group in urea from 1678 cm<sup>-1</sup> to 1629 cm<sup>-1</sup>. This could have been as a result of increased electronegativity of the oxygen atom (with contributions from tautomerism) and a subsequent increase in intra-molecular hydrogen bonding leading to the observed red shift in wavelength. FT-IR analysis of the 3-bromo benzimidazolone polymer showed the presence of Si-O-C bond at about 1085.41 cm<sup>-1</sup>.<sup>34,35</sup> The transmission band was broad with shoulders indicating that there was also contribution from C-H out of plane band. There was also a broad band of N-H bond between 3172–3380 cm<sup>-1</sup> (ref. 32) and there was a shift and a decrease in the intensity of the carbonyl band from 1629 cm<sup>-1</sup> to 1680 cm<sup>-1</sup> as well as a change from C=O to C-O possibly because of the formation of a bond with Si. As a result of increased conjugation, a decrease in intensity and a shift in the C-N band from 1454 cm<sup>-1</sup> to 1499 cm<sup>-1</sup> was also observed.<sup>36</sup> A decrease in the intensity and number of CH out of plane bands of the benzene ring was noticed. This could be attributed to the formation of phenylene units through polycondensation.<sup>36</sup>

### Structure elucidation of 3-bromo benzimidazolone polymer

The <sup>1</sup>H NMR peaks in Fig. 2(a) shows chemical shifts of Ar-H at 6.9 ppm and 7.0 ppm.<sup>37</sup> Chemical shifts at this position is usually due to immobile protons.<sup>38</sup> This therefore suggested

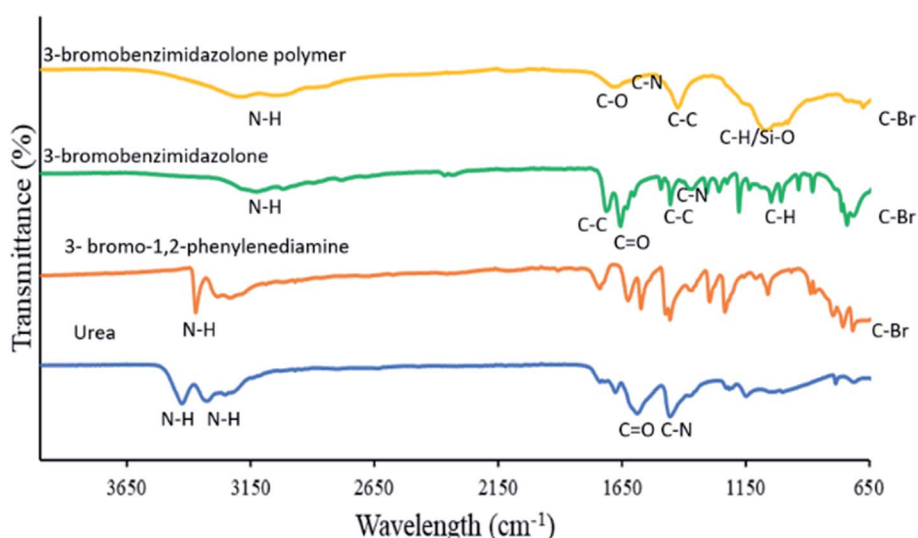


Fig. 1 FTIR spectra for urea, 3-bromo-1,2-phenylenediamine, 3-bromobenzimidazolone and 3-bromobenzimidazolone polymer.



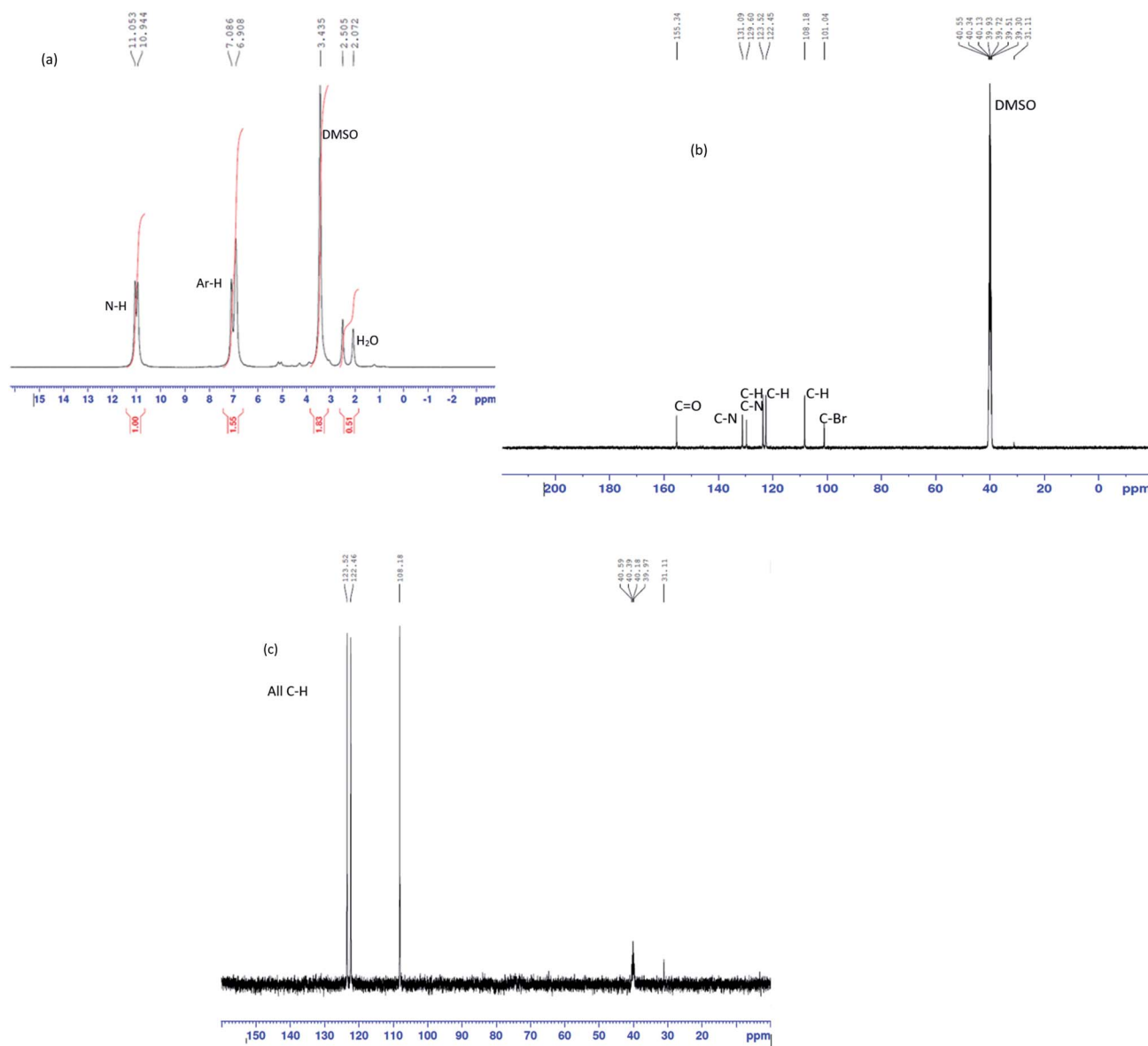


Fig. 2 (a)  $^1\text{H}$ , (b)  $^{13}\text{C}$  and (c) DEPT NMR of 3-bromo-benzimidazolone.

electron redistribution in the benzimidazole ring and confirmed that tautomerism exists in the benzimidazolone ring and could have caused the broad transmission band observed on the IR spectrum for the 3-bromo benzimidazolone. It also shows chemical shifts of N-H at 11.0 and 10.9 ppm.<sup>37</sup> The  $^{13}\text{C}$  NMR peaks on Fig. 2(b) indicated chemical shifts for a total of seven carbon atoms. This is in line with the chemical formula  $\text{C}_7\text{H}_5\text{BrN}_2\text{O}$ , of 3-bromo-benzimidazolone. The chemical shifts were assigned as follows: C=O at 155.3 ppm, C-N at 131.09 ppm and 129.6 ppm, Ar C-H at 123.5 ppm, 122.4 ppm and 108.1 ppm and C-Br at 101.04 ppm.<sup>39</sup> The chemical shifts on the  $^{13}\text{C}$  NMR are confirmed by the DEPT (Fig. 2(c)) chemical shifts. These had all positive amplitudes which indicated that all seven carbon atoms present in the  $^{13}\text{C}$  NMR were CH. The absence of negative amplitudes shows the absence of  $\text{CH}_2$  peaks<sup>40</sup> confirming that all C atoms in the bromo benzimidazolone are unsaturated.

### Morphological studies

As seen in the TEM image (100 nm) of the modified silica (Fig. 3(d)) shows an oily like surface as a result of its recovery from solution. On the SEM image (magnification of 5000 $\times$ ) in Fig. 3(b) pores are evident on the surface of razor-like crystals of silica while the SEM image of the 3-bromo benzimidazolone modified silica (Fig. 3(e)) showed a rough surface with clearly defined pores which shows it could be a good adsorbent. The EDX of the unmodified silica (Fig. 3(c)) shows silicon and oxygen as major elements while the benzimidazolone modified silica (Fig. 3(f)) shows the presence of silicon and oxygen from silica, nitrogen from the benzimidazolone ring and other unreacted elements from the synthesis. This served as extra confirmation of the final product.

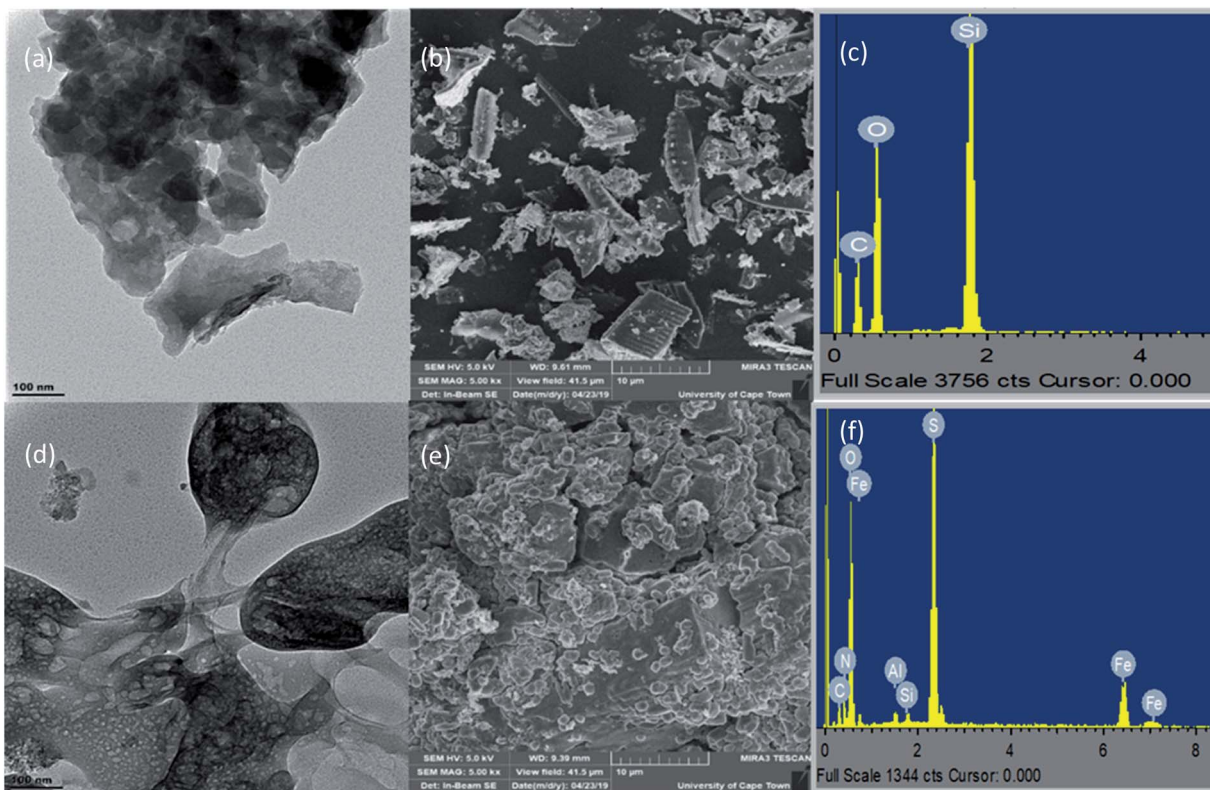


Fig. 3 TEM, SEM and EDX of unmodified silica (a)–(c) and 3-bromo-benzimidazolone modified silica (d)–(f).

### Response surface experiments and model fitting

The quadratic model of the central composite design of the response surface methodology (RSM) was used for modelling experiments altering three reaction parameters: initial oil concentration ( $\text{mg L}^{-1}$ ), adsorbent dosage (g) and contact time (h). The actual percentage removal as calculated using eqn (1) are presented in Table S1.† The colour of the adsorbent treated water had an inverse relationship with the percentage oil adsorption. The more intense the colour, the lower the percentage removal and *vice versa*. However, in experiments carried out with empty tea bags, the colour of the treated water remained the same. This is consistent with results reported by Izevbekhai *et al.*<sup>30</sup> who studied the effect of empty tea bags on oil adsorption. The trends observed in the table are presented in the 3D surface plots.

A graph of model predictions (Fig. 4) of oil removal percentage from synthetic oily wastewater was plotted against the values obtained from experiments. A straight line, with most points distributed on the line and a few very close to the line, was obtained. The coefficient of determination  $R^2$  was found to be 0.99 indicating that the predicting response of the model is good.<sup>41,42</sup>

### Regression model and analysis of variance (ANOVA)

Analysis of variance (ANOVA) was used to find out which of the model terms were statistically significant. The values are presented in Table S2† and summarized in the Pareto chart in Fig. 5. Pareto charts typically highlight the most important

among a large set of data by plotting a series of bar graphs in descending order with the most important factor on the far left. The Pareto chart in Fig. 5 shows that the most significant factors affecting oil adsorption is the initial oil concentration and its quadratic function. Table S2† showed that the quadratic

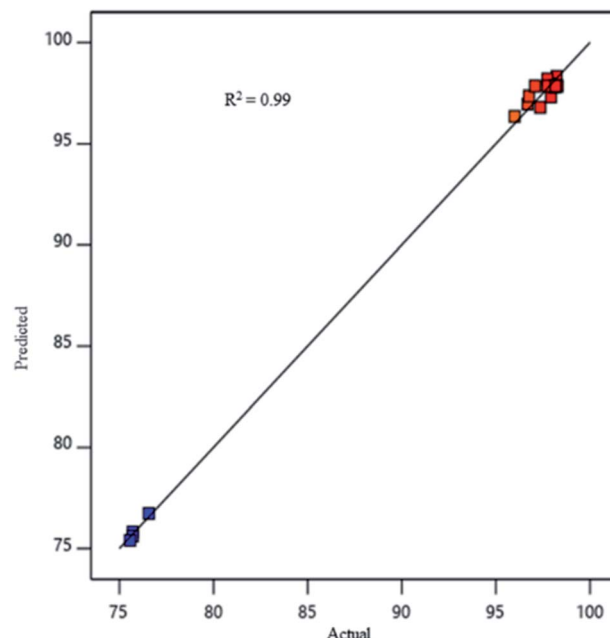


Fig. 4 Comparison between values predicted by response surface methodology (RSM) model and experimentally determined values.

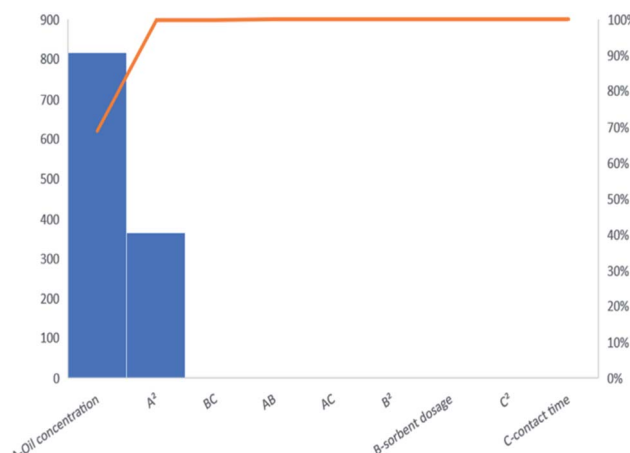


Fig. 5 Pareto charts of contribution of model terms to percentage yield.

polynomial model employed in the representation of percentage adsorption was significant (*p*-value less than 0.05 and high *F*-value) which means that the model was sufficient to represent the design space just like a line of best fit. The lack of fit *P*-value, which was high and therefore not significant, further proved that the model was good. As seen from the Pareto chart, Table S2† also showed that only initial oil concentration and its quadratic function had an effect on the percentage oil removal.

### Effect of oil concentration and sorbent dosage

As the response surface plot (Fig. 6) shows, an increase in initial oil concentration caused an increase in percentage adsorption up to a maximum and started to decrease. This could be because as the oil concentration is increased, larger oil droplets are formed by the coming together of smaller droplets due to the coagulative effect of the adsorbents. These large oil droplets become trapped in the pores of the adsorbent and settle at the base, leaving the water clear.<sup>29,30,43</sup> This could also be because of the introduction of new binding sites as the dosage is increased

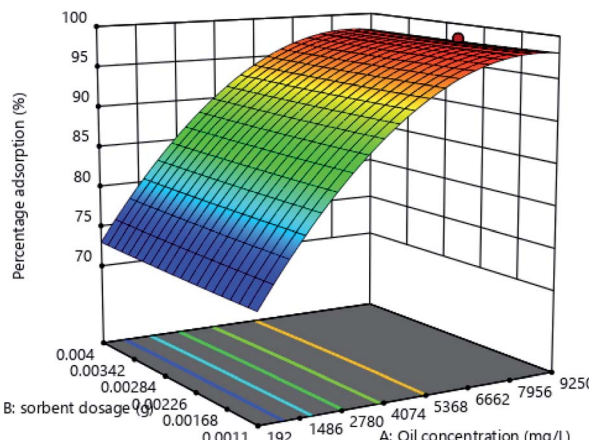


Fig. 6 Response surface plot for the effect of initial oil concentration and adsorbent dosage on percentage adsorption.

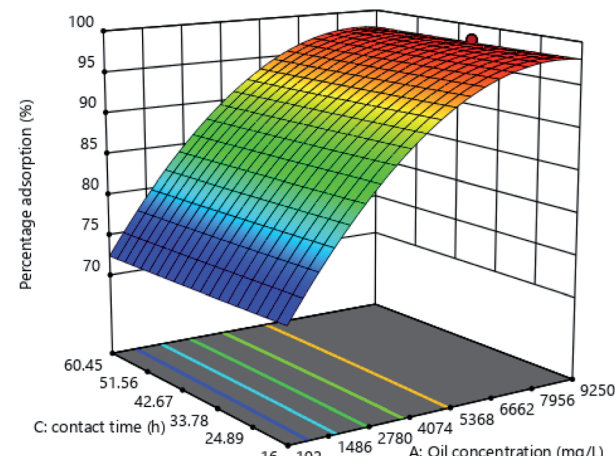


Fig. 7 Response surface plot for the effect of initial oil concentration and time on percentage adsorption.

but as these get saturated, the adsorption capacity begins to reduce.<sup>44–46</sup> With adsorbent dosage, there is a slight increase in adsorption capacity as the adsorbent dosage is increased because of an increase in the binding sites.

### Effect of oil concentration and time

The 3D graph in Fig. 7 shows an increase in percentage oil removal with time. This could be as a result of an increase in the number of positive interactions between the 3-bromo benzimidazolone polymer adsorbent and oil, as the adsorbent stayed in longer contact with the oily solution.<sup>29,30,45</sup>

### Effect of adsorbent dosage and time

As can be seen from the response surface contour plot in Fig. 8, which represents the effect of adsorbent dose and time on

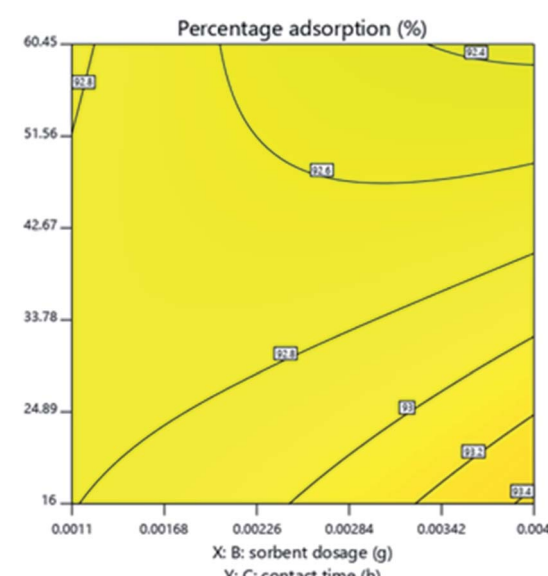


Fig. 8 Response surface contour plot for the effect of contact time and adsorbent dosage on percentage adsorption.



Table 2 Comparison of adsorption capacity for different adsorbents

Adsorbent	Type of oil studied	Sorption capacity (mg g <sup>-1</sup> )	Reference
Silica aerogels	Dibutylphthalate	3500	47
Carbon nanotube polymer composite	Phenol	262	48
Polypyrrole-Si complex	Synthetic oily wastewater (SOWW)	8451	30
Carbon-silica composite	<i>n</i> -Hexane	442	49
3-Bromo-benzimidazolone polymer	SOWW	5196	This study

percentage adsorption, as time and adsorbent dosage increased, the percentage adsorption also increased. The reason for this is, as the dosage was increased, the number of binding sites were also increased and with increase in time, there was prolonged interaction between the oil molecules and the binding sites.<sup>29,30,46</sup>

## Comparison to other similar adsorbents

The adsorption capacity of 3-bromo-benzimidazolone polymer has been compared with other adsorbents in Table 2. As can be seen from the table, the adsorption capacity of 3-bromo-benzimidazolone is comparable to other adsorbents employed in literature. This makes 3-bromo-benzimidazolone a promising adsorbent in the treatment of oily wastewater.

## Conclusions

In this study, 3-bromo-benzimidazolone polymer was successfully synthesized by first synthesizing the benzimidazolone *via* a solvent free process. The synthesized bromo benzimidazolone was then functionalized on pre-extracted silica gels as an oil sorbent material. The oil adsorption performance of this polymer-silica sorbent material in synthetic oily wastewater (SOWW) was then optimized using response surface methodology. It was found that the central composite model chosen was adequate to represent the relationship between the optimized parameters: initial oil concentration, adsorbent dosage and contact time. The results demonstrated that oil removal by adsorption onto benzimidazolone modified silica is feasible. The adsorption and percentage removal were found to be dependent on the adsorbent dose, initial oil concentration and contact time with initial oil concentration being the major determinant of oil adsorption. The optimum conditions for removal of oil from synthetic oily wastewater using silica functionalized with benzimidazolone were as follows 6650 mg L<sup>-1</sup> oil concentration, with adsorbent dosage of 0.004 g and a duration of 16 h. The percentage oil adsorption using these optimum conditions was found to be 97.9%. Given the percentage oil removal, then optimum duration of adsorption and the fact that oil adsorption takes place with stirring or shaking or any form of mechanical agitation, the

benzimidazolone modified silica adsorbent can be applied in field wastewaters. In addition, preliminary studies suggests that mechanical pressure followed by drying at 60 °C gives the adsorbents a potential for regeneration.

## Author contributions

Conceptualization, O. U. I. and W. M. G.; methodology, O. U. I.; software, O. U. I.; investigation, O. U. I.; resources, W. M. G.; writing—original draft preparation, O. U. I., W. M. G. and N. T. T.; writing—review and editing, O. U. I., W. M. G., N. T. T., W. B. A., R. M.; supervision, W. M. G. and N. T. T.; funding acquisition, W. M. G. All authors have read and agreed to the published version of the manuscript.

## Conflicts of interest

There are no conflicts to declare.

## References

- 1 J. M. Wilson and J. M. VanBriesen, *Environ. Pract.*, 2012, **14**, 288–300.
- 2 J. Pichtel, *Appl. Environ. Soil Sci.*, 2016, **2016**, 1–24.
- 3 X. Li, C. Zhang and J. Liu, *Min. Sci. Technol.*, 2010, **20**, 778–781.
- 4 I. M. Cozzarelli, K. J. Skalak, D. B. Kent, M. A. Engle, A. Benthem, A. C. Mumford, K. Haase, A. Farag, D. Harper, S. C. Nagel, L. R. Iwanowicz, W. H. Orem, D. M. Akob, J. B. Jaeschke, J. Galloway, M. Kohler, D. L. Stoliker and G. D. Jolly, *Sci. Total Environ.*, 2017, **579**, 1781–1793.
- 5 X.-N. Cheng and Y.-W. Gong, *Environ. Eng. Res.*, 2018, **23**, 159–163.
- 6 M. Han, J. Zhang, W. Chu, J. Chen and G. Zhou, *Water*, 2019, **11**, 2517.
- 7 S. Noamani, S. Niroomand, M. Rastgar and M. Sadrzadeh, *npj Clean Water*, 2019, **2**, 20.
- 8 M. N. Rashed, in *Organic Pollutants-Monitoring, Risk and Treatment*, ed. M. N. Rashed, InTech Publisher, Rijeka, Croatia, 2013, ch. 7, pp. 167–194.
- 9 L. Yu, M. Han and F. He, *Arabian J. Chem.*, 2017, **10**, S1913–S1922.
- 10 M. K. Dinker and P. S. Kulkarni, *J. Chem. Eng. Data*, 2015, **60**, 2521–2540.



11 H. Moazed and T. Viraraghavan, *Energy Sources*, 2005, **27**, 101–112.

12 H. X. Jin, B. Dong, B. Wu and M. H. Zhou, *Polym.-Plast. Technol. Eng.*, 2012, **51**, 154–159.

13 C. Y. Wang, L. Li and S. X. Zheng, *RSC Adv.*, 2016, **6**, 105840–105853.

14 L. H. Yan and D. F. Zhao, *Arid Environmental Monitoring*, 1998, **12**, 139–144.

15 W. Stöber, A. Fink and E. Bohn, *J. Colloid Interface Sci.*, 1968, **26**, 62–69.

16 I. J. Fernandes, D. Calheiro, F. A. L. Sánchez, A. L. D. Camacho, T. L. A. d. C. Rocha, C. A. M. Moraes and V. C. d. Sousa, *Mater. Res.*, 2017, **20**, 512–518.

17 A. B. D. Nandyanto, F. Iskandar and K. Okuyama, *Chem. Lett.*, 2008, **37**, 1040–1041.

18 O. Izevbekhai, A. Mavrova and K. Anichina, *presented in part at the 13th National Poster Session for Young Scientists, Students and Doctorate Students*, University of Chemical Technology and Metallurgy, Sofia, Bulgaria, 2016.

19 A. Mavrova, K. Anichina, O. Izevbekhai, D. Vutchev, G. Popova-Daskalova, D. Yancheva and S. Stoyanov, *J. Chem. Technol. Metall.*, 2021, **56**, 3–9.

20 S. Samai and K. Biradha, *Chem. Mater.*, 2012, **24**, 1165–1173.

21 H. Lgaz, Y. El Aoufir, Y. El Bakri, A. Zarrouk, R. Salghi, I. Warad, Y. Ramli, A. Guenbour, E. M. Essassi and H. Oudda, *J. Mater. Environ. Sci.*, 2017, **8**, 3290–3302.

22 O. U. Izevbekhai, W. M. Gitari and N. T. Tavengwa, *presented in part at the 20th WaterNet/WARFSA/GWPSA Symposium, Indaba Hotel, Spa & Conference Centre Fourways*, Johannesburg, South Africa, 2019.

23 O. Izevbekhai, W. M. Gitari and N. T. Tavengwa, *S. Afr. J. Chem.*, 2020, in press.

24 B. Shoba, J. Jeyanthi and S. Vairam, *Environ. Technol.*, 2018, 1–16, DOI: 10.1080/09593330.2018.1543353.

25 A. Mavrova, S. Dimov and O. Izevbekhai, *Proceedings of the II-nd International Scientific and Practical Conference - The goals of the World Science*, Dubai, UAE, 2016, vol. 6, pp. 13–15.

26 O. Izevbekhai, K. Anichina-Zarkova, A. Mavrova, D. Vutchev, G. Popova-Daskalova, D. Yancheva and S. Stoyanov, *1st International Balkan Chemistry Congress*, Edirne, Turkey, 2018, vol. 1, p. 237.

27 Z. Yang, J. Wang, L. Li, C. Ye and H. Liu, *J. Heterocycl. Chem.*, 2009, **46**, 788–790.

28 L. Mdlalose, M. Balogun, K. Setshedi, M. Tukulula, L. Chimuka and A. Chetty, *Appl. Clay Sci.*, 2017, **139**, 72–80.

29 O. U. Izevbekhai, W. M. Gitari, A. Wasiu B, N. T. Tavengwa and R. Mudzielwana, *J. Taibah Univ. Sci.*, 2020, **14**, 1033–1041.

30 O. U. Izevbekhai, W. M. Gitari, N. T. Tavengwa, W. B. Ayinde and R. Mudzielwana, *Molecules*, 2020, **25**, 4628.

31 D. S. Ramadhan, Warsito and E. D. Iftitah, *IOP Conf. Ser.: Mater. Sci. Eng.*, 2018, **299**, 012076.

32 A. Abdolmaleki and Z. Bazyar, *Polym.-Plast. Technol. Eng.*, 2013, **52**, 1542–1549.

33 H. Abdeldjebar, Y. Belmiloud, W. Djitli, S. Achour, M. Brahimi and B. Tangour, *Prog. React. Kinet. Mech.*, 2019, **44**, 143–156.

34 A. Kasinathan, R. Rama and G. Sivakumar, *International Journal of Nanotechnology and Applications*, 2010, **4**, 61–66.

35 R. Tian, O. Seitz, M. Li, W. Hu, Y. J. Chabal and J. Gao, *Langmuir*, 2010, **26**, 4563–4566.

36 S. Anand and A. Muthusamy, *J. Mol. Struct.*, 2017, **1148**, 254–265.

37 M. El-Naggar, W. M. Eldehna, H. Almahli, A. Elgez, M. Fares, M. M. Elaasser and H. A. Abdel-Aziz, *Molecules*, 2018, **23**, 1420.

38 D. Zhang and L. Yan, *J. Phys. Chem. B*, 2010, **114**, 12234–12241.

39 D. Smith, *Chemistry of Heterocyclic Compounds: Benzimidazoles and Cogenetic Tricyclic Compounds, Part 1*, 2008, ch. vol. 3, pp. 331–389, DOI: 10.1002/9780470187159.

40 B. Eberhard, *Structure elucidation by NMR in organic chemistry – a practical guide*, John Wiley and Sons Ltd, West Sussex, 2002.

41 J. U. Ani, U. C. Okoro, L. E. Aneke, O. D. Onukwuli, I. O. Obi, K. G. Akpomie and A. C. Ofomatah, *Appl. Water Sci.*, 2019, **9**, 60.

42 L. C. Zhao, J. Liang, W. Li, K. M. Cheng, X. Xia, X. Deng and G. L. Yang, *Molecules*, 2011, **16**, 5928–5937.

43 G. Carlos, C. Juan, S. Wang, G. Luis, R. S. Mohan and S. Ovadia, *SPE Journal*, 2002, **7**, 353–372.

44 N. Syuhada, R. Mohd Ghazi and N. Ismail, *Malaysian Journal of Analytical Sciences*, 2017, **21**, 1101–1110.

45 A. A. Hassan, H. T. Naeem and R. T. Hadi, *IOP Conf. Ser.: Mater. Sci. Eng.*, 2019, **518**, 062003.

46 S. Rahdar, M. Taghavi, R. Khaksefidi and S. Ahmadi, *Appl. Water Sci.*, 2019, **9**, 87–95.

47 R. Filipovic, D. Lazić, M. Perusic and I. Stijepović, *Process. Appl. Ceram.*, 2010, **4**, 265–269.

48 T. A. Saleh, A. Sarı and M. Tuzen, *J. Environ. Manage.*, 2019, **252**, 109660.

49 L. Fu, J. Zhu, W. Huang, J. Fang, X. Sun, X. Wang and K. Liao, *Processes*, 2020, **8**, 372.

